ELSEVIER

Contents lists available at ScienceDirect

Remote Sensing of Environment

journal homepage: www.elsevier.com/locate/rse



Regional-scale hydrological monitoring of wetlands with Sentinel-1 InSAR observations: Case study of the South Florida Everglades



Heming Liao*, Shimon Wdowinski, Shanshan Li

Institute of Environment, Department of Earth and Environment, Florida International University, Miami, FL 33199, United States of America

ARTICLE INFO

Keywords:
Wetland
Everglades
Water level change
SAR interferometry (InSAR)
Tropospheric delay
Gauge
Accuracy

ABSTRACT

Wetland is a very fragile ecosystem that provides important services to a large variety of flora and fauna species, as well as for humans. As wetland depends on water availability, protecting this important ecosystem requires careful hydrological monitoring. The Sentinel-1 mission, featuring a wide swath coverage, high temporal observations and open data policy, provides unprecedented opportunity for high spatio-temporal resolution water level change mapping over regional-wide wetland areas. In this study, we assess Sentinel-1 InSAR observations for routine water level change measurements over the entire south Florida Everglades wetlands. The study utilizes 91 Sentinel-1 images acquired over a three-year period (Sep 2016 to Nov 2019) and generates routine 12-days Interferograms and correspondingly 30 m spatial resolution water level change maps over the entire Everglades. The high spatial resolution interferograms detect hydrological signals induced by both natural- and human-induced flow, including tides, gate operations, and canal overflow; all these cannot be detected by terrestrial measurements. The large number of both InSAR and ground-based gauge observations allow us to quantify the overall accuracy of the Sentinel-1 InSAR measurements, which is 3.9 cm for the entire wetland area, but better for smaller hydrological units within the Everglades. Our study reveals that the tropospheric delay for individual interferograms can be very large, as much as 30 cm (~10 fringes). When applying tropospheric corrections to all three years of Sentinel-1 InSAR observations, the overall accuracy level improved by 13% to 3.4 cm. Although our study is focused on the Everglades, its implications in term of the suitability of Sentinel-1 observations for space-based hydrological monitoring of wetlands and the derived accuracy level are applicable to other wetlands with similar vegetation types, located all over the world.

1. Introduction

Wetlands are very diverse and fragile ecosystems that provide important eco-social services, including flood control, storm protection, water quality maintenance, and ground water recharge (Barbier, 1993). Wetlands are also carbon sequestering systems and, thus, play a significant role in climate regulation (Mitsch et al., 2013; Villa and Bernal, 2018). Over the past century, many wetland areas have been lost, degraded, or stressed mainly due to anthropogenic activities, as water diversion, agricultural development, and urbanization, but also in response to natural processes, as sea level rise and climate change (Davis and Ogden, 1994; Finkl and Charlier, 2003; Sklar et al., 2005). Protection and restoration of wetlands require hydrological monitoring of large areas, as the entire wetland ecosystem depends on its water supply. The commonly used ground-based gauge (water level) measurements provide good temporal resolution, but suffer from poor spatial resolution, as gauge stations are typically distributed several, or

even tens of kilometers, from one another. Furthermore, some remote wetlands have no gauging stations and, consequently, lack critical hydrological information.

Space-based Interferometry Synthetic Aperture Radar (InSAR) monitoring of wetlands has successfully complemented ground-based hydrological observations by providing valuable high spatial resolution measurements of water level changes in both gauged and ungauged wetlands (Brisco et al., 2015; Hong et al., 2010b, 2010a; Hong and Wdowinski, 2014; Jaramillo et al., 2018; Kim et al., 2017, 2014; Lu and Kwoun, 2008; Wdowinski et al., 2008; Wdowinski, 2004). Insofar, wetland InSAR studies, which were based on previous generations of SAR satellites, demonstrated the great potential of InSAR for wetland water level monitoring, but also pointed at the limitation of the technique mainly due to limited data availability. Previous SAR satellite missions have acquired data with 30–100 km wide swath, repeat orbit of 11–45 days, and inconsistent acquisition policy. Consequently, SAR data over wetlands covered narrow areas with infrequent temporal

E-mail address: heming.liao@outlook.com (H. Liao).

^{*} Corresponding author.

coverage. For example, wetland InSAR studies of the south Florida Everglades mainly focused on limited areas and were based on a limited number of acquisitions, typically less than 20 (e.g., Wdowinski et al., 2004, 2008; Hong et al., 2010b, 2010a).

Sentinel-1, which is a constellation two SAR satellites launched in 2014 and 2016, respectively, represents a new generation of SAR satellites that acquire data consistently over most land areas every 6 or 12 days with a 250 km wide swath. Moreover, all data from these two satellites are free. The short revisit cycle, wide swath coverage, as well as the free and open data policy, provide an unprecedented opportunity to conduct regular water level change monitoring over wide wetland areas.

This study expands upon our previous InSAR wetlands studies of the south Florida Everglades (e.g., Wdowinski et al., 2004, 2008; Hong et al., 2010b, 2010a), by analyzing a large dataset of Sentinel-1 scenes acquired systematically almost every 12 days over a three-year period. We chose to focus on the Everglades, because these wetlands can be viewed as a large-scale testing ground for space-based hydrological monitoring, due to the variety of wetland types (marshes, swamps, mangrove forests), variety of hydrological regimes (controlled, natural flow), and a dense network of gauging stations. Unlike the previous studies, which were limited in spatial and temporal coverages, the current study investigates hydrological changes throughout the entire Everglades wetlands with 12 days temporal resolution, allowing us to detect spatial and temporal water level change patterns in a systematic manner over a three-year period. Furthermore, our systematic analysis enables us to conduct quality assessment of the Sentinel-1 based observations, in term of measurement accuracy for each hydrological regime and the entire Everglades wetlands. In addition, we address the issue of tropospheric delay and its impact on InSAR-based water level change measurements by applying tropospheric delay corrections. We also discuss the advantages and limitations of Sentinel-1 derived water level change products and their implications for water management, hydrological modeling, and hydro-ecology applications in the Everglades and other wetland areas, worldwide.

2. Study area

The Everglades is a wetland prairie (also named 'a river of grasses' by Douglas (1947)) that covers an approximate $100~\rm km \times 160~\rm km$ area extending from the Everglades Agriculture Area to the margin of the Florida Bay and Gulf of Mexico (Fig. 1(a)). The Everglades support a variety of vegetation and wetland types, including swamps, marshes, and mangrove forests. Anthropogenic changes in the past century, mainly for water supply, agricultural development and flood control purposes, have disrupted natural water flow.

The current Everglades consists of both flow-controlled and natural flow areas, which are divided into seven hydrologic units shown in Fig. 1(a). The flow control areas are divided into five Water Conservation Areas (WCA1, WCA2A, WCA2B, WCA3A and WCA3B). The natural flow areas include the Big Cypress National Preserves (BCNP) and the Everglades National Park (ENP). The overall water level follows the elevation pattern of the Everglades, which is characterized by a general north-south gradient in the inland wetlands and a northeast-southwest gradient in the coastal wetlands along the Gulf of Mexico, as shown in the elevation map (Fig. 1(b)).

Water levels in the flow-controlled and naturally flow areas have different spatial patterns. Water flow in the controlled region is divided and separated by canals and levees, which often lead to discontinuity in water levels between neighboring areas. For the necessity of water management, pumps and gate structures were built along the boundaries of these controlled areas. The operation of these control structures causes water level in these areas to be more dynamic and sometimes characterized by high water level gradient. Due to water management activities, water level differences in adjacent hydrologic units can reach over 1 m (Palaseanu and Pearlstine, 2008). In natural flow areas, water

level gradients are usually low following the low-gradient topography, resulting in an overall sheet-flow behavior of surface water (McVoy et al., 2011). Water levels are also affected by seasonal variations due to precipitation and evapotranspiration. In the wet season (July to December), water levels are usually high due to large precipitation; while in the dry season (January to June), water levels are relatively low and sometime below the surface. Water level along the southwest coast can show large variation in sub-daily time periods due to tidal fluctuation.

3. Datasets

This study relies mainly on two data types, the Sentinel-1 SAR data and ground-based water level data measured by gauge stations. The ground-based data are used for both calibration and validation of the space-based observations.

3.1. SAR data

The Sentinel-1 constellation (Sentinel-1A and Sentinel-1B) satellites are instrumented with C-band (radar frequency of 5.4 GHz) SAR sensors, which work in all weather conditions, day and night. Each Sentinel-1 satellite has a 12-days revisit cycle and the constellation of the two satellites provides a 6-days repeat cycle. Although the satellites can acquire data using four different acquisition modes, the systematic data acquisition has been conducted mostly with the Interferometric Wide (IW) swath mode, using the Terrain Observation with Progressive Scans (TOPS) technique. The IW mode acquires data with a 250 km wide swath at 2.3 m by 14 m spatial resolution (single look). Although Sentinel-1 data are acquired in both HV and VV polarizations, we used only VV polarization, because it maintains higher signal-to-noise-ratio compared to HV polarization over the Everglades (Hong and Wdowinski, 2012).

We used a total of 91 Sentinel-1 acquisitions, which were acquired over the Everglades since the operation of the first satellite in September 2015 until November 2019 (Fig. 1(c)). For the first years from September 2015 to September 2016, Sentinel-1 acquisitions were temporally sparse. Since September 2016, a consistent data acquisition plan was maintained over our study area, except for some small gaps between April 2017 and August 2017. Out of the 91 acquisitions, only 89 were acquired by the Sentinel-1A sensor and the remaining 2 by Sentinel-1B. The timeline of data acquisition over south Florida is shown in Fig. 1(c). The coverage of the Sentinel-1 SAR data is shown in Fig. 1(a), which is consisted of two concatenated adjacent Sentinel-1 scenes (blue rectangles shown in Fig. 1(a)). More detailed Sentinel-1 data information is provided in the supplementary Tables S1 and S2.

3.2. Hydrological data

Another important dataset used in this study is water level measurements acquired by more than 300 gauges stations over the entire Everglades (Fig. 1(b)). The gauge stations provide near real time water level measurements, which are available online by the Everglades Depth Estimation Network (EDEN - https://sofia.usgs.gov/eden/). Most gauge stations provide hourly water level measurements, but some stations provide only daily mean measurements. In our study, we used all hourly measurements from about 210 gauges within the seven hydrological units.

4. Methodology

4.1. Wetland InSAR

InSAR is proven to be an effective tool for detecting surface water level change over floodplains and wetlands (Alsdorf et al., 2001a, 2001b; Alsdorf et al., 2000; Lu et al., 2005; Wdowinski et al., 2004). The technique relies on double-bounce scattering (Richards et al.,

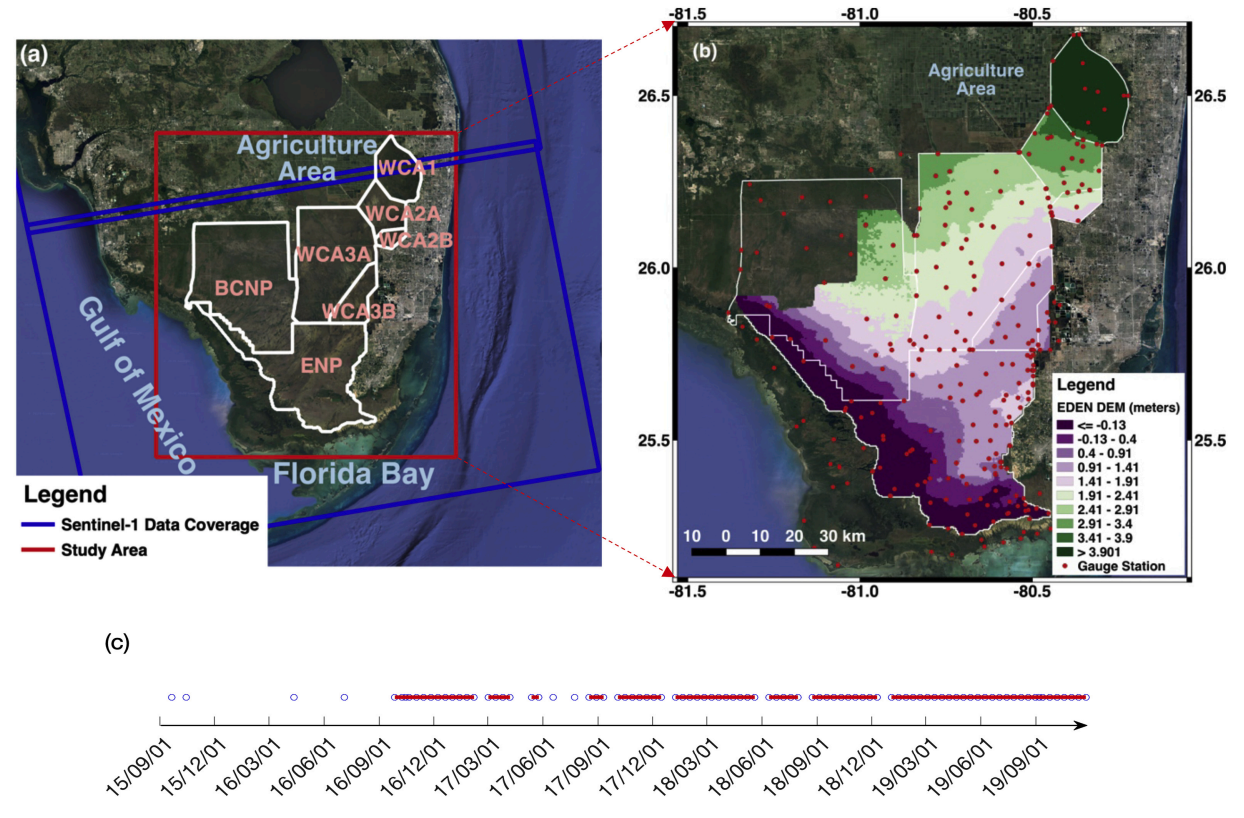


Fig. 1. (a) Location map of the study area (red rectangle), the main hydrologic units (marked by white polygons), and Sentinel-1 data coverage (blue rectangle) overlaid on a Google Earth image of South Florida. (b): Everglades elevation (source: EDEN DEM, NAVD88, Oct 2011) and gauge stations distribution (red dots) overlaid on google satellite image. (c) Sentinel-1 data acquisition and InSAR data pair combinations. Blue circles represent the dates of Sentinel-1 acquisition and solid red lines mark the interferometric pairs used in the study. There are 74 12-days Interferograms for over three years period (September 2016 – November 2019). (For interpretation of the references to colour in this figure legend, the reader is referred to the web version of this article.)

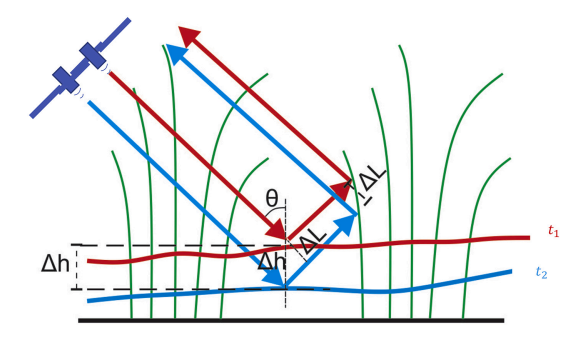


Fig. 2. Schematic illustration showing the geometry of SAR scattering in wetland environment and its change with time. Δh represents water level change between SAR data acquisitions at times t_1 and t_2 ; ΔL is the corresponding oneway range change in the line of sight between the satellite and the water surface; θ is the incidence angle of the SAR data acquisition.

1987), which occurs through the interaction of radar signal with the water surface and emergent shrubs or vegetation (Wdowinski et al., 2004). A schematic illustration of scattering geometry in wetlands and its use for water level change detection is shown in Fig. 2.

We present a simple case of water level change occurring between two SAR data acquisitions at times t_1 and t_2 . The vertical water level change (Δh) results in a line of sight (LOS) path length change of ΔL between the satellite and the surface, which is determined by the measurement incidence angle (θ) . Based on the geometric relations shown in Fig. 2, the relation between ΔL and Δh are:

$$\Delta h = \frac{\Delta L}{\cos \theta} \tag{1}$$

InSAR measures phase changes ($\Delta \emptyset$) in the LOS direction, which can be converted to length using the SAR sensor wavelength (λ), as follows:

$$\Delta L = \frac{\Delta \emptyset}{4\pi} \lambda \tag{2}$$

By combining both eqs. (1 and 2), water level change (Δh) can be calculated based on the measured InSAR phase as follow:

$$\Delta h = \frac{1}{\cos \theta} \cdot \frac{\Delta \emptyset}{4\pi} \lambda \tag{3}$$

In SAR interferometry, the measured phase $\Delta\varnothing$ is a summation of several contributing components, including the flatten earth phase $(\Delta\varnothing_{flat})$, topographic phase $(\Delta\varnothing_{topo})$, ionospheric advance $(\Delta\varnothing_{iono})$, tropospheric delay phase $(\Delta\varnothing_{tropo})$, water level induced hydrological phase $(\Delta\varnothing_{hydro})$ and noise $(\Delta\varnothing_{noise})$.

$$\Delta \emptyset = \Delta \emptyset_{flat} + \Delta \emptyset_{topo} + \Delta \emptyset_{iono} + \emptyset_{tropo} + \Delta \emptyset_{hydro} + \Delta \emptyset_{noise}$$
(4)

The accuracy of water level change measurements is highly dependent on our ability to accurately separate hydrological interferometric phase change ($\Delta \oslash_{hydro}$) from other processes that affect phase change between the two SAR acquisitions.

The flatten earth phase ($\Delta \varnothing_{flat}$) and the topography phase ($\Delta \varnothing_{topo}$) can be removed easily with high accurate orbit information and accurate DEM, which is typically available nowadays. The atmospheric component mainly consists of ionospheric phase advance and tropospheric phase delay. For C-band Sentinel-1 SAR data, ionospheric delay is usually negligible in mid-latitude regions, such as our study area (Liang et al., 2019; Meyer, 2010; Meyer et al., 2016); thus ionospheric delay is ignored in our study. The tropospheric component is the largest error source in InSAR measurements and requires special considerations. For accurate hydrological phase $\Delta \varnothing_{hydro}$ estimate, it is important

to minimize the noise effect and remove, as much as possible, the tropospheric effect. We will describe our processing strategy for generating high quality InSAR phase $\Delta\varnothing$ in Section 4.2 and dealing with tropospheric phase delay (\varnothing_{tropo}) effect in the sections 4.3.

4.2. InSAR data processing

Sentinel-1 Interferograms are generated following the instructions in Wegnüller et al. (2016). Following that, we conducted flatten earth curvature and topographic phase removal. The topographic phase is removed using the 1/3 arc National Elevation Dataset (NED) Digital Elevation Model (DEM) from the United States Geological Survey (USGS). Due to decorrelation and noise effects, the topographic corrected interferogram can still be noisy. A multi-look number of 10×2 in range and azimuth were used, in order to reduce noise, but still maintain a relative fine spatial resolution of about 30×30 m² for water level products. To further reduce noise effect, we applied the classic Goldstein adaptive spectrum filter (Goldstein and Werner, 1998) with an alpha exponent of 0.5 and a filtering window size of 64 pixels. Finally, we used the Minimal Cost Flow (MCF) algorithm for phase unwrapping (Werner et al., 2002).

4.3. Tropospheric delay analysis

Tropospheric phase delay, which is one of the major error sources in InSAR measurements, introduces noise into water level change measurements. In previous wetland InSAR studies, tropospheric effect was identified as a potential error source (e.g., Hong et al., 2010b, 2010a), but not quantitatively addressed. Because the noise associated with tropospheric phase delay increases with the lateral scale of the study area (Hanssen, 2001), tropospheric induced noise is more significant in our regional-scale study of the entire south Florida peninsula than previous studies, which focused on smaller areas.

There are different approaches accounting for the tropospheric effects in InSAR, among which meteorological reanalysis and numerical weather models based InSAR tropospheric correction have become a common practice due to global data availability and increasing temporal-spatial resolution. We explored two software packages the Python based Atmospheric Phase Screen Estimation (PyAPS) (Jolivet et al., 2011) and the Generic Atmospheric Correction Online Service (GACOS) (Yu et al., 2018a, 2018b; Yu et al., 2017), including three weather models (ECMWF and MERRA model from PyAPS, and the ECMWF operational model from GACOS), to evaluate the tropospheric effect for InSAR water level change estimate. We compared Interferograms with and without tropospheric correction and assessed the correction performance by comparing the troposphere corrected InSAR derived water level changes to independent ground-based gauge measurements.

4.4. Sentinel-1 InSAR for water level change measurements

4.4.1. From InSAR phase change to water level change measurements

To convert InSAR phase change measurements to water level changes, the results need to be calibrated, because InSAR measurements are relative in both space and time. InSAR measures phase change between two acquisitions ($\Delta \oslash = (\oslash_2 - \oslash_1)$) with respect to phase change of a reference point ($\Delta \oslash_{ref}$). We use gauge water level measurements as a reference to calibrate our results. An alternative method for calibrating the relative InSAR measurements of water level changes relies on radar altimetry observations, which provide independent hydrological information in ungauged wetlands (Kim et al., 2009; Yuan et al., 2017).

The calibration procedure of the unwrapped InSAR phase change include two steps: (1) unwrapped LOS phase change conversion to vertical water level change; and (2) calibration of InSAR derived water level change with gauge measurements. The conversion of the unwrapped LOS phase changes to water level changes is conducted for

each 30 \times 30 m² pixel following Eq. (3). InSAR and gauge measurements are then extracted at each gauge locations. InSAR measurements (Δh_{InSAR}) at each gauge location are calculated by the mean value of 9 (3 \times 3) pixels with the gauge station location as its center. Accordingly, we extract gauge water levels (h_1 , h_2) corresponding to InSAR data acquisition times (t_1 , t_2) and their differential value ($\Delta h = h_1 - h_2$). As the gauge measurements are conducted with an hour temporal resolution, a direct gauge measurement corresponding to the SAR image acquisition time does not exist and, thus, the gauge measurements (h_1 , h_2) were calculated using linear interpolation of neighboring time measurements. The final step of the calibration analysis is estimation of the reference point phase change (offset) parameter, using a least square liner fit analysis with a single parameter (Kim et al., 2009; Wdowinski, 2004), as follows:

$$\Delta h_{Gauge} = \Delta h_{InSAR} + offset \tag{5}$$

where Δh_{Gauge} and Δh_{InSAR} are the gauge and InSAR derived water level change measurements, respectively.

The offset parameter is then added to the InSAR measurements to retrieve the corrected water level change results as following:

$$calibrate_{\Delta h_{InSAR}} = \Delta h_{InSAR} + offset$$
 (6)

In other InSAR applications, as earthquake or volcano related deformation, the reference point is typically selected in the far field, where the deformation is assumed to be negligible (Massonnet et al., 1993), and the deformation field is assumed to be continuous from the reference point to all other points. However, the continuous phase change assumption is not valid when using InSAR for measuring phase changes induced by water level changes across flow barriers, such as levees separating the various hydrologic units in the Everglades. Water level changes within different hydrologic unit can vary independently and can be discontinuous. Thus, the calibration needs to be conducted separately for each hydrologic unit. In our study, the calculation of the offset parameter was conducted separately for each of the water conservation areas (WCA1, WCA2A, WCA2B, WCA3A, WCA3B), which are separated by canals or levees. As the natural flow hydrologic units (ENP and BCNP) are not disturbed by levees or canals, we calculated a single offset parameter for both areas.

The calibration procedure worked well in the comparison of most InSAR and gauge stations, but not in all locations due to limitations of the InSAR observations or unusual hydrological conditions. Therefore, we eliminated some of the unreliable InSAR observations using the following criteria: (1) We excluded InSAR measurements at gauge locations characterized by low interferometric coherence, typically in areas of open water. In our analysis, a threshold of 0.5 was used to exclude low coherence measurements. In some locations of low coherence, we managed to include InSAR observations, by applying a virtual station approach to extract the value from its nearby reliable patch (Hong et al., 2010b, 2010a). (2) We exclude observations during the dry season, in which gauge measures are below ground water level changes, whereas InSAR measures no changes on the surface. Gauge measurements representing a subsurface water level measurement are automatically detected in our processing as the property of this data is marked as 'dry' in the gauge metadata. In our data analysis, we noticed that some of gauges do not have surface elevation measurement and, as a result, these gauges may not be properly labeled as 'dry' when the measurement actually represents a below surface water level. Large discrepancy can happen if these dry gauge measurements are not properly identified and excluded. We manually checked suspicious gauges and exclude these measurements by comparing with them to surrounding gauges that have surface elevation measurements. (3) We excluded some gauges located outside levees boundary, which do not represent water levels inside the levees. (4) We excluded dynamic gauge measurements, especially those near water operation structures. For gauges showing large variations in short time periods due to water structure operation (Lin and Gregg, 1988) and, the interpolation result

most likely do not represent the true value. (5) We removed obvious outliers, which are characterized as extremely large values comparing to their surrounding measurements.

4.4.2. Accuracy assessment

With calibrated InSAR-derived absolute water level changes, we assess their accuracy by comparing them to gauge measurements. A Root Mean Square Estimate (RMSE) was calculated for each interferogram by comparing the calibrated InSAR derived water level changes with the gauge measurements. The overall accuracy of Sentinel-1 InSAR measurements, was calculated from all 12-days Sentinel-1 InSAR observations that cover a period of about three years. Similarly, the same accuracy analysis was applied and calculated for each hydrologic unit.

5. Results

Our study yielded several results types, including interferograms, tropospheric corrected interferograms, calibrated water level maps, and accuracy assessment of the InSAR-derived water level change measurements. We first present examples of calculated interferograms showing their ability to detect high spatial resolution hydrological signals (Sections 5.1) and representative interferograms that were used to derive water level change maps and accuracy estimates (Section 5.2). We then present examples for tropospheric phase delay and its correction (Section 5.3) and representative calibrated water level change maps (Section 5.4). Finally, we analyze all three years 12-days Sentinel-1 InSAR derived water level change maps for calculating the statistical tropospheric effect and the overall InSAR water level change maps accuracy (Section 5.5).

5.1. An example Sentinel-1 Interferogram reflecting water level changes

An example 12-day interferogram shows an overall organized phase change patterns in the water conservation areas (WCA1, WCA2A, WCA3A) and diffused fringe patterns in the naturally flow areas of the ENP and BCNP (Fig. 3(a)). Most fringes in WCAs terminate sharply along the edge of the WCAs. In some WCAs, fringes are divided by levees, canals, roads, as observed in WCA3A, where the fringes in the northern part of the area are affected by the Miami canal. Several radial fringe patterns located along some of the WCAs boundaries are shown in Fig. 3 (a1) (a2). The fringes in natural flow areas (BCNP and ENP) are less organized, except of an elongated fringe located inland of the southwest coast of the ENP (Fig. 3 (a3)). There are also three diffuse fringes located along the east coast of south Florida in urban area.

Fringe patterns in both WCAs and naturally flow areas reflect changes in hydrological conditions that occurred between the two acquisition dates (2016/10/09 and 2016/10/21). In contrast, we attribute the three diffused fringes located in the urban area to the tropospheric phase delay, because urban area is not expected to have phase changes (deformation) over a 12-days period. Fringe termination along WCA boundaries verifies that InSAR measurements primarily represent the water level changes, as the wavelength of tropospheric delay is usually much longer, as can be observed by the three fringes over the urban area. Visible fringe features along man-made structures, such as levees, canals, roads also suggest that the origin of the phase variation is due to the hydrological water level variations. Sentinel-1 InSAR observations also provide rich information of other hydrological activities over the Everglades. For example, the dense fringe patterns in WCA1, WCA2, WCA3 reflect water structure operation (Wdowinski et al., 2004, 2008). Fig. 3(a1) shows three interesting parallel radial phase patterns, which are caused by the gate operation shortly after the hurricane Mathew poured heavy rain in October 2016. Another interesting feature is the double-radial fringe pattern presented in Fig. 3(a2), which also occurred due to gate operation. The elongated coastal-parallel fringes occur along the transition between fresh- and saltwater vegetation (Fig. 3(a3)) and mark the edge of the tidal flushing zone (Wdowinski et al., 2013). The few fringes over natural flow areas of the ENP and BCNP represent remnant of the sheet flow due to small elevation gradient.

5.2. Sentinel-1 InSAR for water level change measurements over entire Everglades

Two examples are used below to explain the procedures for generating water level change maps from interferometric unwrapped phase changes and their accuracy evaluation. The first example is a wet season interferograms (Interferograms 20160927–20161009 Fig. 4(a)). The InSAR-derived water level change estimates in the LOS direction are first converted to vertical water level change map following Eq. (3). As presented in Section 4.4, vertical water level changes can be discontinued due to the separation of levees or canal and, thus, are calibrated independently for the estimate of the offset parameter in each hydrological unit (WCA1, WCA2A, WCA2B, WCA3A, WCA3B, ENP + BCNP). The calibration constant (offset parameter) estimates are shown in Fig. 4(b), in which unreliable InSAR vs gauge measurements were excluded based on the criteria summarized in Section 4.4. Calibrated water level change products are calculated with the estimated offset parameter following Eq. (6). In order to calculate the InSAR uncertainty level of the entire study area, we combined all calibrated InSAR-gauge measurements into a single scatter plot and calculate the RSME of the combined dataset (Fig. 5(c)). The RMSE analysis indicates a fit level of 2.6 cm, indicating a very good agreement between the InSAR and the gauge measurements of water level changes.

A second example of converting an interferogram to a hydrological data is from the dry season (20170113–20170125), when the natural flow areas, BCNP and ENP, are very likely to dry out and water level could drop to below surface. In this case, a large number of InSAR vs gauge estimates can have large discrepancies. The dry season example interferogram present a low gradient fringe pattern in both natural flow and controlled areas (Fig. 5(a)). The final InSAR vs gauge measurement scatter plot shows only a limited number of valid InSAR-gauge pairs, as many data points are excluded due to the dry hydrological conditions, in which water level are below ground level (Fig. 5(b)). The RMSE of this example (2.7 cm) is similar to the RMSE of the wet season example (2.6 cm). Scatter plots of remaining 72 interferograms are included in supplementary Fig. S2.

5.3. Tropospheric correction examples

In order to reduce tropospheric delay errors in InSAR measurements of water level changes, we applied tropospheric corrections provided by GACOS and PyAPS and evaluated their quality using the procedure described in Section 4.4.2. Our analysis found that the ECMWF operational model based tropospheric estimate from GACOS provides a better estimate in terms of capturing the shape and retrieving the correct magnitude of the tropospheric delay than that the ECMWF and MERRA model-based estimates from PyAPS. This finding agrees well with recently published results (Murray et al., 2019). Here we only present the tropospheric delay estimates provided by GACOS. We first present three examples, in which the impact of tropospheric corrections can be evaluated visually (Fig. 6) and then provide quantitative assessments of the correction quality (Fig. 7). The original 12-day interferograms are termed OCT (20181023-20181104), NOV (20181104-20181116) and JAN (20190103-20190115). All three interferograms are characterized by a long wavelength fringe patterns that interfere with the shorter wavelength, which are characterized by high fringe gradients observed in the WCAs (Fig. 6). The long wavelength fringe patterns vary from one interferogram to the other. In the OCT interferogram the long wavelength signal roughly oriented E-W (Fig. 6(a1)), in the NOV interferogram the orientation is roughly NE-SW (Fig. 6(b1)), and in the JAN interferogram the long wavelength has a concave shape, roughly

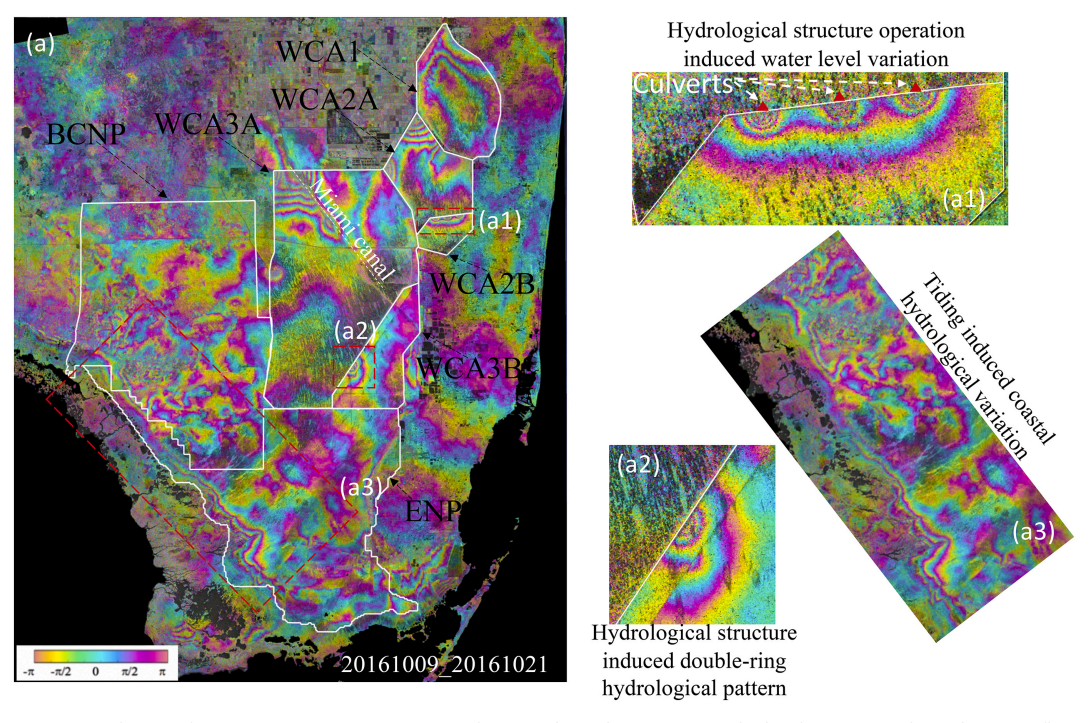


Fig. 3. A representative Sentinel-1 Interferogram (20161009–20161021) showing phase change over south Florida. (a) Most phase changes reflect surface water level change, but also tropospheric phase delay. The white solid lines mark the boundaries of the hydrologic units (WCA1, WCA2A, WCA2B, WCA3B, BCNP, ENP). Interesting hydrological signal are marked by red dash boxes are enlarged in figures (a1), (a2), and (a3). Each fringe cycle (from red to yellow to green to blue and back to red) in the interferogram represents a 3.6 cm vertical elevation change. All interferograms presented in the following share the same colour scale as presented here. (For interpretation of the references to colour in this figure legend, the reader is referred to the web version of this article.)

following the shape of the Florida coastlines (Fig. 6(c1)).

These large tropospheric signals interfere with the hydrological signal and should be removed, in order to extract more accurate water level measurements. As described in Section 4.3, we extracted the GACOS tropospheric phase delay for each interferogram, as shown in the middle column of Fig. 6. We noticed that the tropospheric estimates provided by GACOS include high spatial frequency variations (noise). Thus, we applied a median and average filter to suppress the high frequency noise but keep the low frequency, long wavelength tropospheric signal. The GACOS filtered tropospheric phase delays (middle column in Fig. 6), show very similar fringe patterns and magnitudes to those in the original interferograms (left column in Fig. 6).

The troposphere corrected interferograms were calculated by subtracting the GACOS tropospheric estimates from the original interferograms (right column of Fig. 6). Visually, the improvement after the tropospheric correction is clear, as less long wavelength signal are reduced or even completely removed. This is especially obvious for the OCT and JAN examples, in which the hydrological patterns stand out after the tropospheric correction.

A quantitative analysis of the tropospheric correction performance is conducted by comparing InSAR to gauge water level measurements with corrected and uncorrected interferograms. Visually, the InSAR vs gauge measurements deviate from the 1-by-1 dash line before the tropospheric correction (Fig. 7). The deviation is especially obvious in the NOV comparison (Fig. 7(a1) and 7(a3)). With the tropospheric correction, all three cases show significantly better fit to the 1-by-1 dash line. The RMSEs reductions are 65.8%, 23.7%, and 40.5% for the OCT, NOV, and JAN datasets, respectively.

5.4. Representative water level change maps

We generated 72 (out of a total of 74) 12-days interferograms and converted them to maps of water level change covering the entire Everglades. We excluded two interferograms, which were almost

completely decorrelated. In some of the 72 good interferograms, we also masked areas with low interferometric coherence (below 0.5 in the filtered interferogram), in order to eliminate unreliable results. Here we present two representative maps, one for wet season (20161009–20161021 - Fig. 8(a)), and the other for the dry season (20170113–20170125 - Fig. 8(c)). We chose to present these maps, because they contain interesting hydrological signals or possible processing artifacts, marked by five boxes and two polygons in Fig. 8. The maps also show different hydrological characteristics between the wet and dry seasons. For evaluating the quality of the InSAR-based maps, we compare them to water level changes maps calculated from the differences of EDEN water level surfaces (Figs. 8(b) and 8(d)), which are obtained from the interpolation of 300+ gauge measurements (Fig. 1(b)), for the same InSAR acquisition dates.

The InSAR-derived water level change map (Fig. 8(a)(c)) and gauge interpolated maps (Fig. 8(b)(d)) show an overall good agreement at most areas, in terms of magnitude and spatial patterns of water level change. This similarity is most apparent in the WCAs and can serve as an indicator quality of Sentinel-1 InSAR for water level change mapping over the entire Everglades. However, in a few locations, the InSAR- and gauge-derived maps show variations or disagreements with one another, especially for the dry season data. The differences between InSAR- and gauge- derived maps are mainly attributed to the measurements' spatial resolution, temporal resolution, observation type, and data processing errors.

InSAR-derived water level change map has a higher spatial resolution (30 m) than that of gauge interpolated maps (nominal resolution 400 m, actual resolution varies in the range of 1–10 km according to gauge station distribution (Fig. 1(b)). Thus, some hydrological signals are detected by InSAR but not the gauge-derived maps. For example, in Fig. 8(a) box 1, the InSAR-based map shows a narrow pattern of water level change occurring along the Miami Canal (Fig. 3(a)), which is not detected in the interpolated EDEN gauge-based water level maps (Fig. 8(b)). In Fig. 8(a) Box 2, the InSAR-based map shows three small-

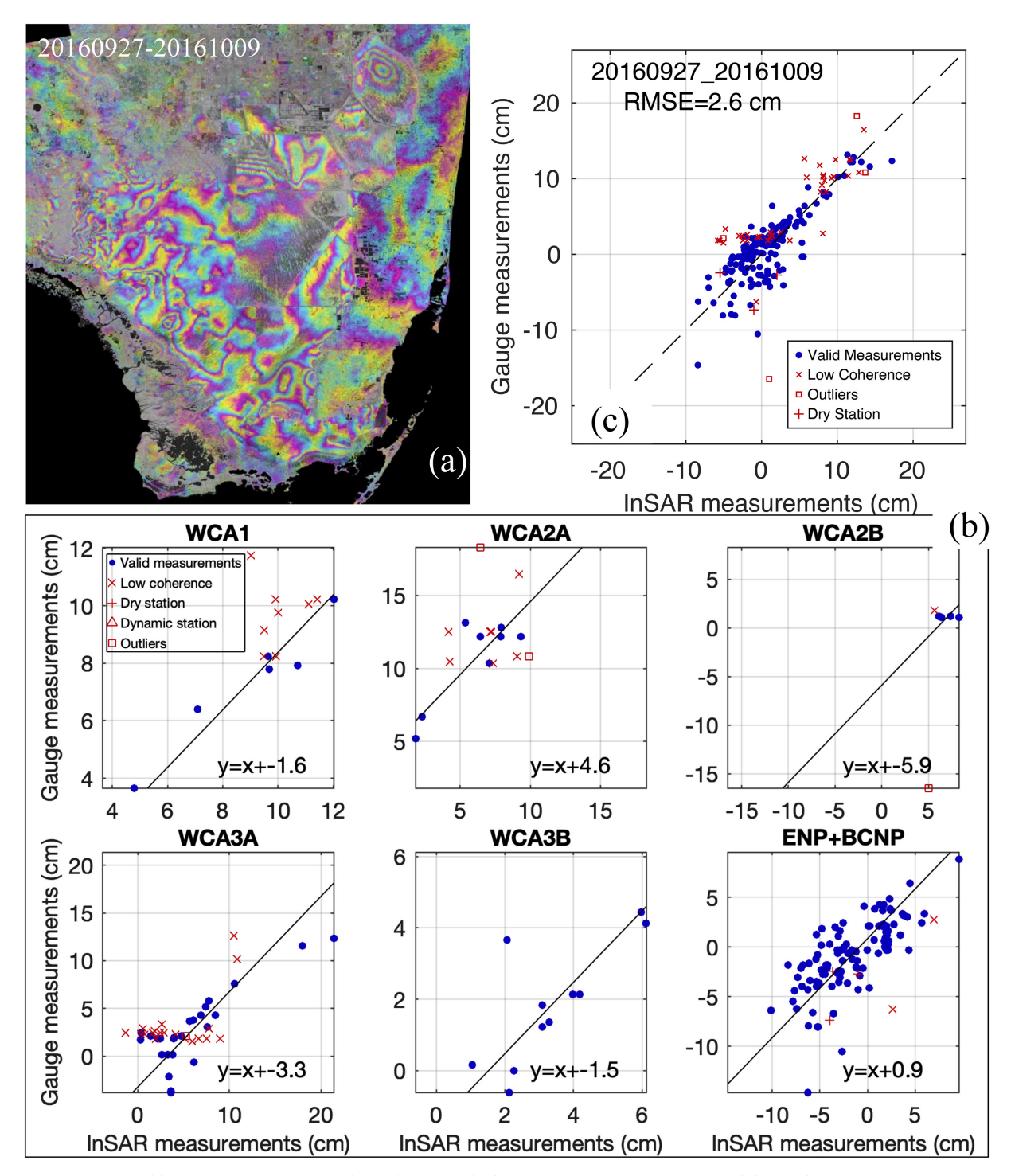
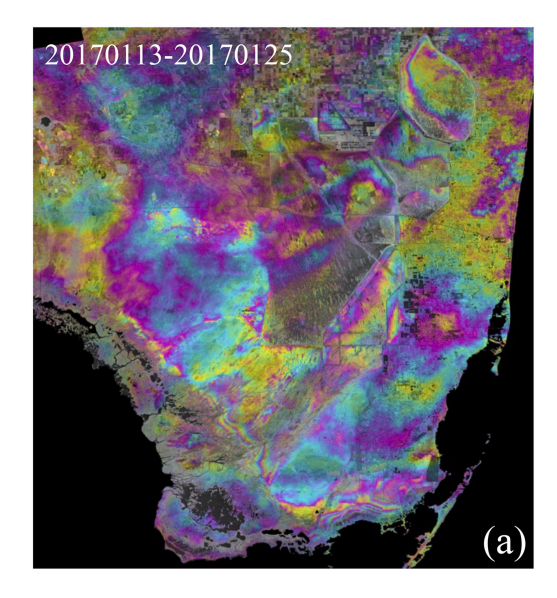


Fig. 4. An interferogram, calibration plots, and error analysis of an example data (20160927–20161009) acquired during the wet season. (a) Interferogram. (b) Scatter plots of InSAR vs gauge measured water level changes, the best fit line with slope 1, and estimated offset parameter for each hydrological unit. (c) Scatter plot of all reliable InSAR vs gauge water level change measurements and its RMSE estimate for all hydrological units.

scale (2–3 km) radial water level change patterns centered at three hydrological structures, culverts (S144_T, S145_T, S146_T, shown as magenta triangle in Fig. 8(a) in box 2 and in Fig. 3(b)), whereas the EDEN-based map doesn't provide such details. In addition, the gauge interpolation map shows a strange pattern in WCA2B, due to the limited number of gauges (Fig. 1(b)) in the area.

InSAR-derived water level change maps represent water level differences between two specific times (InSAR image pair acquisition times), whereas gauge-based maps represent water level differences between two EDEN water level surfaces for the same InSAR image acquisition dates; each EDEN water level surface was derived from interpolation of daily median gauge measurements. Thus, areas with dynamics water level, such as the coastal area influenced by sub-daily tides, the two maps show significant variations. For example, in Fig. 8(a) Box 4, InSAR derived water level change show a large coastaligned water level change, which does not appear in EDEN derived map (Fig. 8(b)).

Another factor contributing to the difference between the InSARand gauge-derived maps arise from the different observation abilities. Gauge measures both above and below surface water level and, hence,



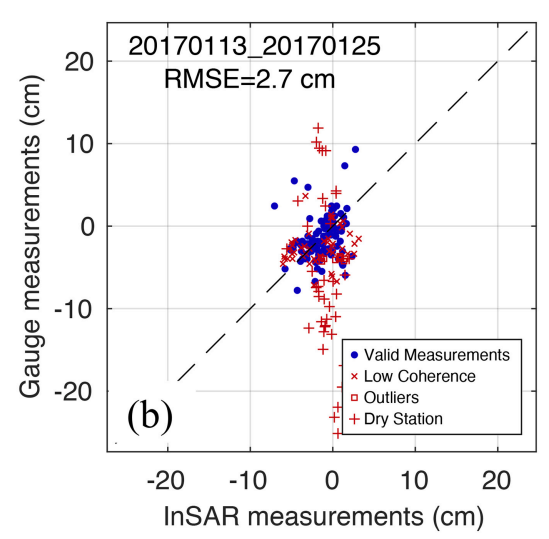


Fig. 5. Interferogram and error analysis of an example data (20170113–20170125) acquired during the dry season, (a) Interferogram. (b) Scatter plot of all reliable InSAR vs gauge water level change measurements and its RMSE estimate for all hydrological units.

the gauge-based interpolation is sensitive to water level changes both above and below the surface, whereas InSAR measures only surface water level changes. Hence, when water level drops below the surface, InSAR- and gauge- derived water level change maps can show significant differences. For example, Fig. 8(b) Box 3, the EDEN gauge-derived water level change shows large magnitude variations within the box area, whereas the InSAR derived changes are small (Fig. 8(a)). The verification of this discrepancy is presented in the Fig. S2 in the Supplementary Materials. Similar discrepancies between InSAR- and Gauge-derived water level changes can be detected in the BCNP and ENP areas during the dry season and are attributed to below ground measurements of the gauge stations (Fig. 8(c)(d)).

Data processing errors, as phase unwrapping, can contaminate InSAR-derived water level change maps. For example, in Fig. 8(a) Box 5, the InSAR derived water level change map shows large variation from the EDEN gauge result at two stand-out yellowish patches, which were caused by a phase unwrapping error.

The dry season InSAR-derived map shows smaller amplitude and lower gradients of water level changes (Fig. 8(c)) compared with the gradients in the wet season water level change map (Fig. 8(a)). Even in dry season, water conservation areas (WCA1, WCA2, WCA3) are still covered with water and, hence, InSAR successfully detects water level change variations, that are constrained by the boundaries of these hydrological units. The InSAR derived water level change at the ENP and BCNP areas are very small, as the water level in most of these two regions are below surface. Two other discrepancies between the InSARand gauge-derived water level changes in the dry season maps were detected in ENP and are marked by dashed black lines (polygons -Fig. 8(c)). In polygon 1, InSAR water level change map shows a long tail feature, located along the Shark River Slough, which is at relatively low elevation. The detection of water level changes suggests that the area is covered by surface water even during the dry season. Polygons 2 is located along the coastal margin and represents water level changes induced by coastal tides (Fig. 8(c)), which is not detected by the daily mean values used to calculate the EDEN gauge-derived map (Fig. 8(d)).

In this section we presented only two examples of the InSAR derived water level maps. The other 72 such maps are presented in the Fig. S3 in the Supplementary Materials. As InSAR detects only surface water level changes, InSAR-derived water level change maps usually match well with gauge interpolation measurements during the wet season, when water level is relatively high and above the surface. During the dry season, when water level is low and can reach below surface levels,

InSAR- and gauge-derived maps can have large discrepancies. The InSAR-derived maps are still good, as they represent surface water level changes.

5.5. Accuracy analysis of InSAR-based water level change measurements

To gain an overall accuracy estimate of the three years InSAR measurements over the entire Everglades, we conducted a statistical analysis using validation points, where InSAR- and gauge-base measurements of water level changes are compared. We first calculated the InSAR measurement accuracy of each InSAR-derived water level change map using all reliable InSAR-gauge pairs using the same scattering analysis presented in Fig. 4(c) and 5(b). We conducted the analysis for 72 out of 74 interferograms (2 datasets are completely decorrelated and are excluded), by calculating the RMSE of the InSARgauge misfit with and without atmospheric correction (Fig. 9). The analysis reveals that 72% of datasets yield an equal or decreased RMSE values with tropospheric correction. The remaining 28% datasets result in RMSE increase with tropospheric correction. However, all the increased RMSE values are less than 2 cm and only two datasets experience an RMSE increase larger than 1 cm. With the tropospheric correction, 76% of the InSAR water level change maps have an RMSE smaller than 4 cm.

We calculated the overall accuracy of all 72 InSAR-derived water level change maps by adding all reliable InSAR-gauge values of each individual map into combined scatter plots (Fig. 10). The RMSE calculations of all validation points reveal an InSAR accuracy level of 3.9 cm without tropospheric correction (Fig. 10(a)) and 3.4 cm with the correction (Fig. 10(b)). The results indicate a roughly 13% accuracy improvement when using the ECMWF operational model (GACOS) based tropospheric corrections.

6. Discussion

The quantitative analysis of about three-year long Sentinel-1 dataset demonstrates the capability of using Sentinel-1 InSAR observations for water level change monitoring of a wide wetland region with frequent, every 12-day, acquisitions. Our study is focused on the south Florida Everglades wetlands, as it provides a wealth of ground-based hydrological observations, which are essential for evaluating the space-based observations. However, our results are applicable to many other wetlands around the world, which have similar vegetation types.

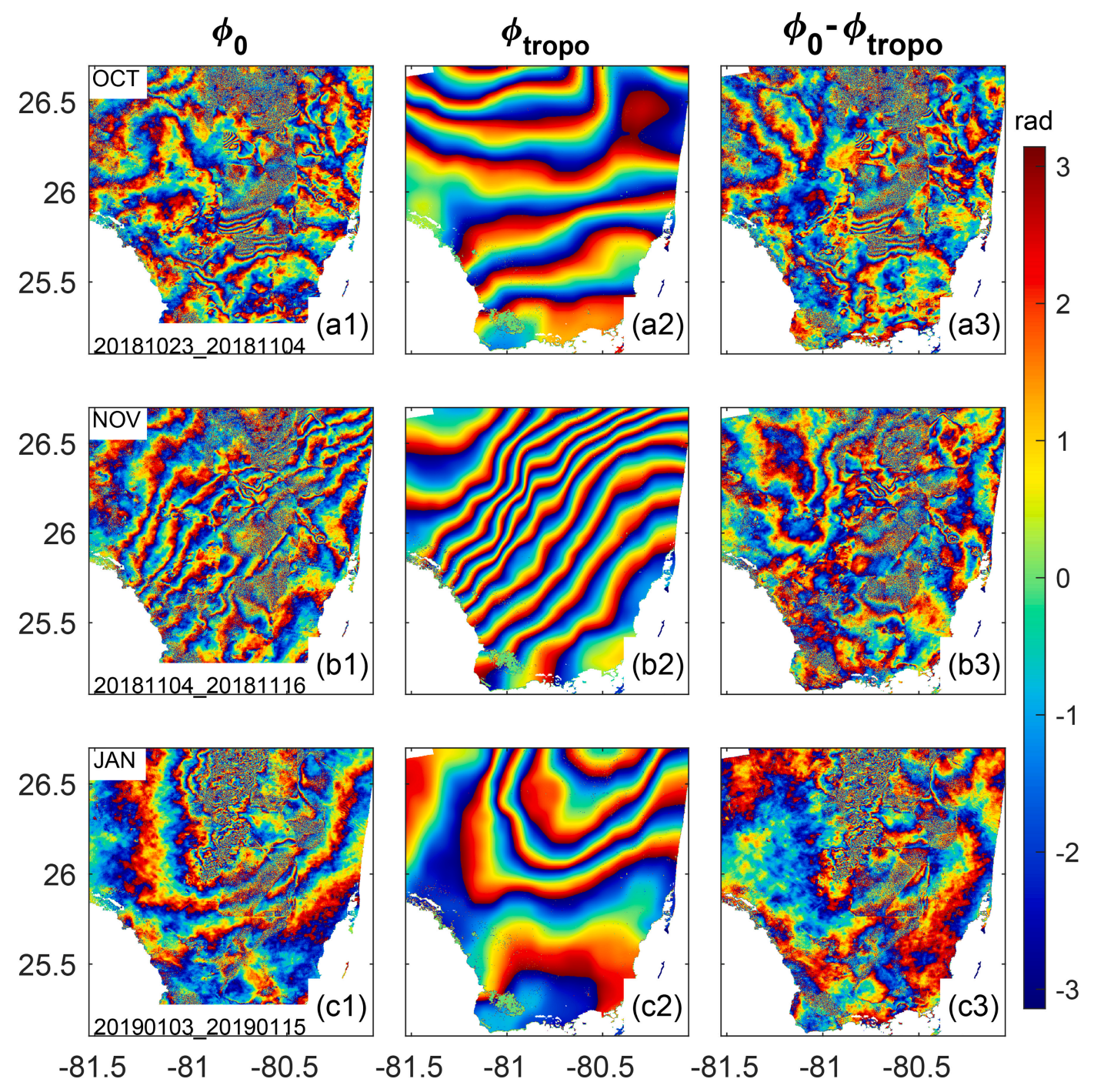


Fig. 6. Three examples of wetland InSAR Tropospheric correction implementation. The left column shows the original interferograms \varnothing . The middle column shows the filtered LOS differential tropospheric delay estimates \varnothing_{tropo} provided by GAOCS. The right column shows the tropospheric corrected interferograms $\varnothing - \varnothing_{tropo}$

6.1. Regional-scale hydrological monitoring

Our study revealed that Sentinel-1 InSAR data are very suitable for regional-scale monitoring of water level changes over the entire Everglades. Previous studies also explored the suitability of InSAR for detecting water level changes with other SAR sensors, including TerraSAR-X (Hong et al., 2010b, 2010a), RADARSAT (Brisco et al., 2015; Hong et al., 2010b, 2010a; Hong and Wdowinski, 2012; Kim et al., 2009), ERS-1/2 (Lu et al., 2005; Lu and Kwoun, 2008), ENVISAT (Zhang et al., 2016), ALOS (Hong et al., 2010b, 2010a; Kim et al., 2009; Lu et al., 2009) and JERS-1 (Wdowinski et al., 2004, 2008). However, these previous studies were mainly designed for evaluating the

potential of InSAR for wetland water level change detection due to narrower acquisition swath (several tens of km) and limited data availability. The main reasons for lacking time series analysis is decorrelation effect due to longer repeat orbit of previous C-band missions (24 days of Radarsat-1/2 and 35 days of ERS-1/2 and Envisat) and inconsistent data acquisition policy. The reliable 12-day repeat acquisitions with 250 km wide swath coverage enabled us, for the first time, to monitor water level changes in the Everglades in a consistent manner. New and upcoming SAR missions, which include the Canadian RADARSAT Constellation (launched in May 2019) and the NISAR mission (scheduled launch in 2022), will provide more frequent InSAR acquisitions for a consistent space-based monitoring of water level

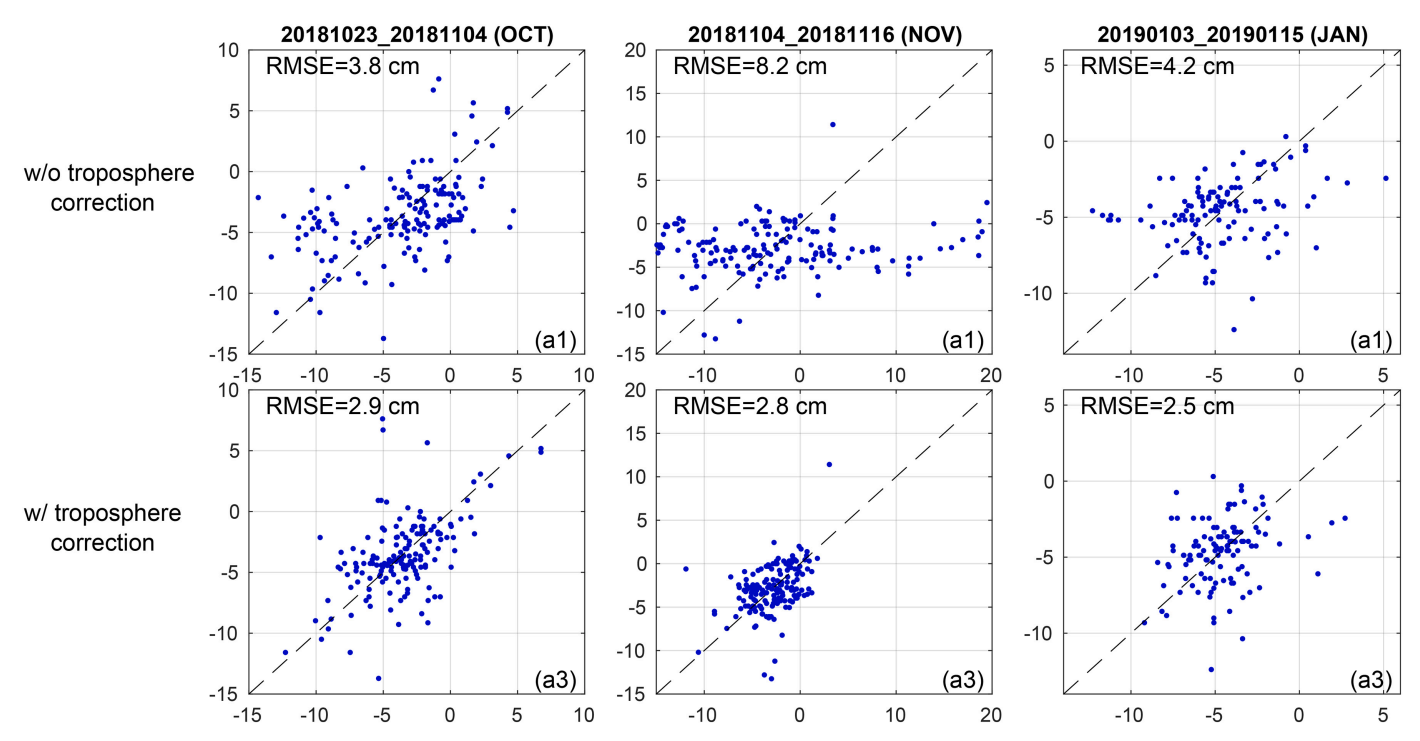


Fig. 7. Scatter plots of InSAR-derived vs EDEN gauge water level change measurements, without tropospheric correction (first row) and with tropospheric correction (second row). The dashed line marked the theoretical 1-by-1 line.

changes over the Everglades.

6.2. InSAR accuracy dependency on hydrological units' characteristics

Our scattering analysis revealed that the accuracy of InSAR-based water level change measurements over the entire Everglades is 3.9 cm without tropospheric correction and 3.4 cm when applying the correction (Section 5.5). However, when applying the same scattering analysis to subset of InSAR-gauge validation points according to hydrologic units, we found that the accuracy level, as defined by RMSE, vary in the range of 1.7–4.4 cm, as shown in Fig. 11. Overall, we found better accuracy levels within the water conservation areas (WCAs). Most water conservation areas have an accuracy in the range 1.7–3.3 cm; whereas the accuracy of the natural flow area ENP is 3.4 cm and 4.4 cm for BCNP area, as shown in Fig. 11.

The different accuracy level among the various hydrologic units can be attributed to several possible reasons, including vegetation types, hydrological conditions, and lateral dimension of the hydrologic units. First, the vegetation distribution over the different hydrologic units varies from mostly herbaceous vegetation in the WCAs, to a mixture of herbaceous and woody vegetation in the ENP, to mostly woody vegetation in BCNP. These structural differences in vegetation affect the scattering mechanism and, hence, may affect the InSAR observation quality. For example, studies in South Florida with ALOS-1, ERS-1/2 (Kim et al., 2013) and Eastern Canada with Radarsat-1 (Brisco et al., 2017) found that woody vegetation areas (e.g. cypress, mixed shrubs swamp) usually have higher coherence comparing with herbaceous vegetation (sawgrass, graminoid), as there are more return signal due to double bounce from the vegetation trunks, branches, stems. Second, the presence and level of surface water also result in scattering behavior of the vegetation (Costa, 2004) and, consequently, impact InSAR observation quality. Water levels in the WCAs are typically higher than in the naturally flow areas (Pearlstine et al., 2007), resulting in stronger double-bounce scattering when vegetation is inundated compared with weaker single-bounce scattering in dryer conditions (Alsdorf et al., 2001a, 2001b; Brisco et al., 2017). Finally, the lateral dimension of the hydrologic units can also affect the accuracy level, because InSAR uncertainty level due tropospheric phase delay increases with lateral distances (Emardson et al., 2003). Although we used multiple gauge stations for calibrating the InSAR-based measurements instead of a single reference point, the accuracy of the measurements still depends and decreases with horizontal distances within each hydrologic unit.

6.3. Tropospheric effect for wetland InSAR

Our study reveals that the tropospheric noise can be significant when using Sentinel-1 InSAR observations for wetland water level change detection. The tropospheric delay in most interferograms vary in the range of 3-5 cm per hydrologic unit, but it can be as large as 28 cm (10 fringes) across the entire everglades, as shown in Figure 6b2. Unlike other InSAR deformation studies, such as urban subsidence and post-seismic deformation, in which deformation usually vary slowly over time, water level changes in wetlands are very dynamic (time scale of hours to days) due to tide, rainfall and water management activity. Thus, tropospheric delay is often inseparable from hydrological signal when using InSAR time series techniques, such as short baseline subset InSAR or permanent scatter InSAR techniques (Li et al., 2019). We find that the ECMWF operational model based tropospheric delay products provided by GACOS can mitigate the tropospheric delay effectively. The effectiveness of GACOS-based InSAR tropospheric correction can attribute to: (1) short time difference between the ECMWF product (24:00) and the Sentinel-1 acquisition (~23:28) over the Everglades, and (2) high spatial resolution of the new ECMWF product (0.125 degree), which accounts for both long and intermediate wavelength tropospheric changes.

6.4. Limitation

The calculated InSAR-derived high spatial resolution water level change measurements cannot be obtained by any terrestrial-based methods. However, the InSAR observations are still limited in their accuracy and hydrological implementation. Our scattering analysis revealed an accuracy level of 1.7–4.4 cm with respect to the ground-based gauge measurements after applying tropospheric correction. Possible

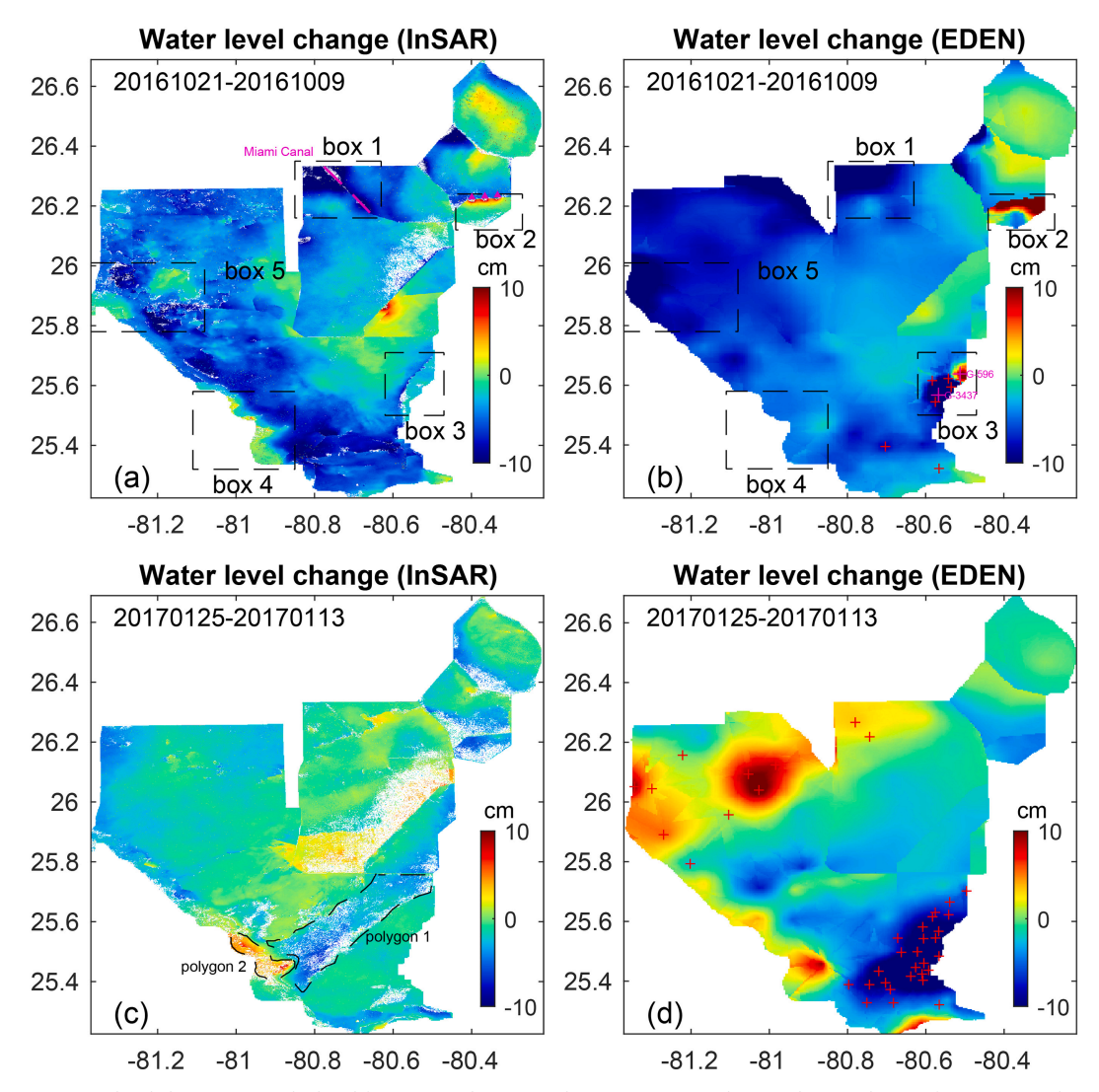


Fig. 8. Representative water level change maps calculated from Sentinel-1 InSAR observations ((a) and (c)) and interpolation of EDEN gauge data ((b) and (d)). The upper row presents maps for the period 20161009 and 20161021 (wet season), whereas the lower row presents maps for the period 20170113 and 20170125 (dry season).

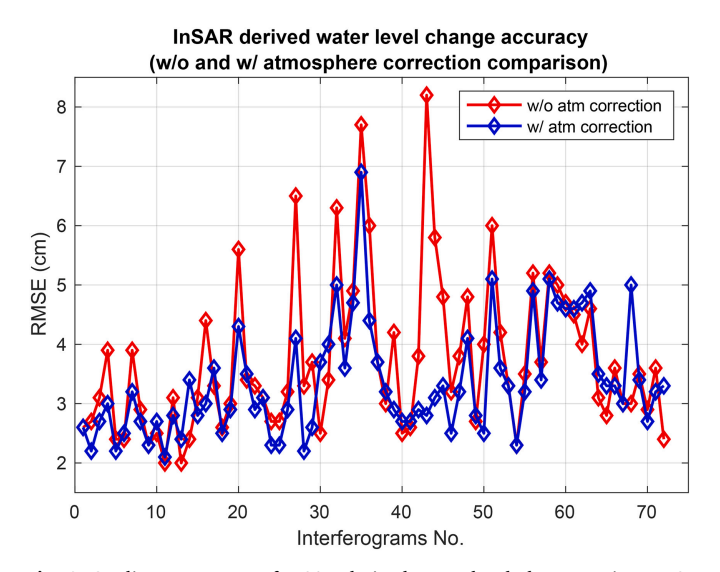


Fig. 9. Quality assessment of InSAR derived water level changes using RMSE calculations with and without troposphere correction for 72 InSAR derived water level change maps.

error sources that can explain the misfit between InSAR and gauge measurements may arise from unmodeled, including smaller lateralscale tropospheric delay, phase unwrapping, and decorrelation; understanding these error sources requires additional research, which is beyond the scope of this study. The limited implementation of InSARderived water level change maps by hydrologists reflect the relative nature of the InSAR measurements of water level changes between two SAR acquisition times, instead of 'absolute' water level desired by hydrologists. A possible way to convert the current water level change maps to absolute water level measurement is to seek external datasets for calibration. Hong et al., 2010b, 2010a used gauge measurements and assumed flat water level conditions at the end of the wet season, as a reference water surface for calculating successive water level surfaces using InSAR observations. Future work can used similar ground-based gauge observations or space-based altimetry observations (such as the recently launched ICESAT-2 altimetry) for both calibrating the InSAR observations and converting them to absolute water levels.

7. Conclusions

The wide swath, high spatial-temporal resolution characteristic of Sentinel-1 SAR observations combined with open and free data policy has opened up great opportunities for using InSAR for region-scale

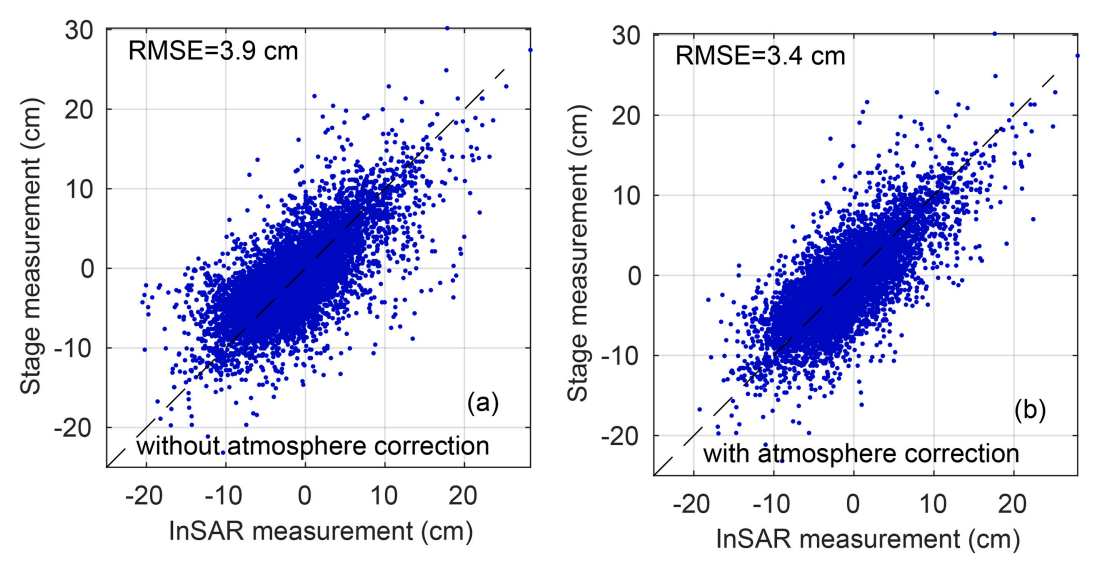


Fig. 10. Accuracy estimates of multi-temporal InSAR-derived water level change measurements without (a) and with (b) tropospheric correction. The accuracy is estimated from RSME calculations using a scattering anlysis of all reliable InSAR-gauge water level change measurements of each of the 72 InSAR-derived maps, as presented in Fig. 4(c) and Fig. 5(b).

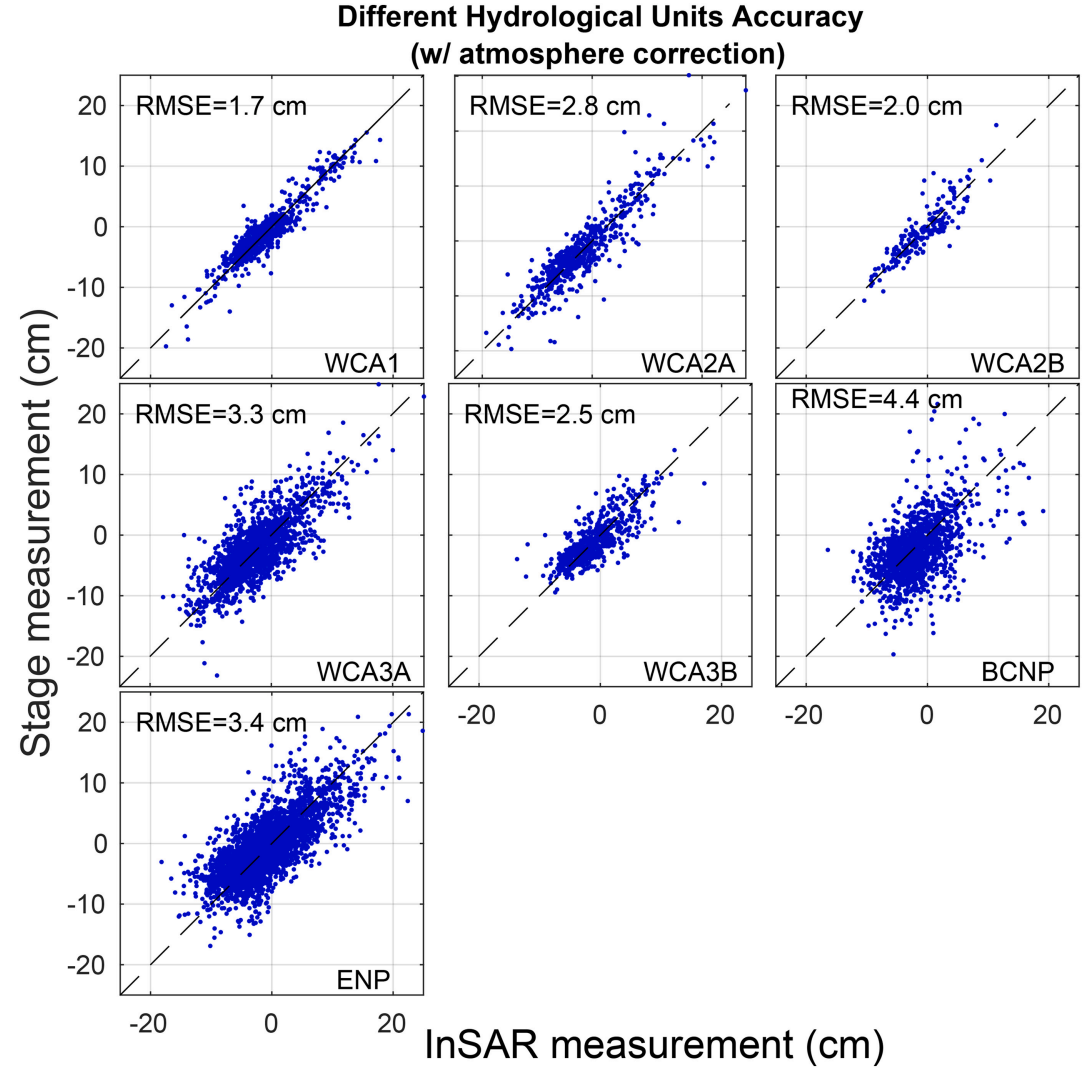


Fig. 11. Scatter plots of InSAR- vs gauge-derived water level change measurements and their accuracy estimate for each hydrological unit. The InSAR measurements where obtained from all 72 water level change maps calculated with tropospheric correction. The accuracy is estimated from RSME calculations using all reliable InSAR-gauge water level change measurements.

wetland water level change mapping. We examined the feasibility of using Sentinel-1 InSAR observations for space-based hydrological monitoring of the entire Everglades wetlands in south Florida. Our study generated high spatial resolution (30 m) maps of water level changes that occurred over the entire Everglades during a 3+ year period. The water level change maps detected several detailed spatial hydrological features, including radial flow patterns induced by gate operations, water overflow from a canal to its surroundings, and water level changes in the tidal zone. These maps could be of great data sources for water management practice, hydrology modeling and ecohydrology applications. With over three years of InSAR observations, our study reveals that the troposphere corrected InSAR-based water level change measurements have an overall accuracy of 3.4 cm for the entire study area. We also determined the InSAR accuracy level for each hydrological unit in the Everglades and found that the accuracy level is higher for the flow-controlled areas (1.7-3.3 cm) compared with the natural-flow areas (3.4-4.4 cm). Our study shows that tropospheric effect can be significant, in the range of several cm up to 28 cm, for individual Sentinel-1 InSAR-based water level change estimate. By implementing tropospheric corrections to all three years datasets, the accuracy level improved by 13%. Upcoming SAR mission, as the NISAR mission, will provide additional and more frequent InSAR observations that will allow more frequent space-based monitoring of water level changes in the Everglades and other wetland areas around the world.

Credit author statement

Conceptualization, Methodology: Heming Liao, Shimon Wdowinski; Data processing, Writing- Original draft preparation: Heming Liao.

Results analysis/interpretation, paper revision: Heming Liao, Shimon Wdowinski, Shanshan Li.

Supervision and Funding: Shimon Wdowinski.

Declaration of Competing Interest

The authors declare that they have no known competing financial interests or personal relationships.

that could have appeared to influence the work reported in this paper.

Acknowledgement

We thank two anonymous reviewers for the thoughtful comments, which helped us to improve the quality of this manuscript. We also thank the European Space Agency and the Alaska Satellite Facility Distributed Active Archive Center (ASF DAAC) for providing the Sentinel-1 SAR data. We also thank Newcastle University for providing the GACOS InSAR troposphere products (http://ceg-research.ncl.ac.uk/v2/gacos/) and the Everglades Depth Estimation Network (EDEN) for providing the gauge water level measurements. This study was supported by NSF grant #DEB-1832229. It is contribution number 980 from the Southeast Environmental Research Center in the Institute of Environment at Florida International University.

Appendix A. Supplementary data

Supplementary data to this article can be found online at https://doi.org/10.1016/j.rse.2020.112051.

References

- Alsdorf, D., Birkett, C., Dunne, T., Melack, J., Hess, L., 2001a. Water level changes in a large Amazon lake measured with spaceborne radar interferometry and altimetry. Geophys. Res. Lett. 28, 2671–2674.
- Alsdorf, D.E., Melack, J.M., Dunne, T., Mertes, L.A.K., Hess, L.L., Smith, L.C., 2000. Interferometric radar measurements of water level changes on the Amazon ood

- plain. 404. pp. 4
- Alsdorf, D.E., Smith, L.C., Melack, J.M., 2001b. Amazon floodplain water level changes measured with interferometric SIR-C radar. IEEE Trans. Geosci. Remote Sens. 39, 423–431.
- Barbier, E.B., 1993. Sustainable use of wetlands valuing tropical wetland benefits: economic methodologies and applications. Geogr. J. 22–32.
- Brisco, B., Murnaghan, K., Wdowinski, S., Hong, S.-H., 2015. Evaluation of RADARSAT-2 acquisition modes for wetland monitoring applications. Can. J. Remote. Sens. 41, 431–439. https://doi.org/10.1080/07038992.2015.1104636.
- Brisco, B., Ahern, F., Murnaghan, K., White, L., Canisus, F., Lancaster, P., 2017. Seasonal change in wetland coherence as an aid to wetland monitoring. Remote Sens. 9, 158. https://doi.org/10.3390/rs9020158.
- Costa, M.P.F., 2004. Use of SAR satellites for mapping zonation of vegetation communities in the Amazon floodplain. Int. J. Remote Sens. 25, 1817–1835.
- Davis, S., Ogden, J.C., 1994. Everglades: The Ecosystem and its Restoration. CRC Press. Douglas, M.S., 1947. The Everglades: river of grass Sarasota, FL. Pineapple Press, Inc 1988, 310.
- Emardson, T.R., Simons, M., Webb, F.H., 2003. Neutral atmospheric delay in interferometric synthetic aperture radar applications: statistical description and mitigation. J. Geophys. Res. Solid Earth 108.
- Finkl, C.W., Charlier, R.H., 2003. Sustainability of subtropical coastal zones in southeastern Florida: challenges for urbanized coastal environments threatened by development, pollution, water supply, and storm hazards. J. Coast. Res. 934–943.
- Goldstein, R.M., Werner, C.L., 1998. Radar interferogram filtering for geophysical applications. Geophys. Res. Lett. 25, 4035–4038.
- Hanssen, R.F., 2001. Radar Interferometry: Data Interpretation and Error Analysis. Springer Science & Business Media.
- Hong, S.-H., Wdowinski, S., 2012. Evaluation of the quad-polarimetric Radarsat-2 observations for the wetland InSAR application. Can. J. Remote. Sens. 37, 484–492. https://doi.org/10.5589/m11-058.
- Hong, S.-H., Wdowinski, S., 2014. Multitemporal multitrack monitoring of wetland water levels in the Florida Everglades using ALOS PALSAR data with Interferometric processing. IEEE Geosci. Remote Sens. Lett. 11, 1355–1359. https://doi.org/10.1109/ LGRS 2013 2293492
- Hong, S.-H., Wdowinski, S., Kim, S.-W., Won, J.-S., 2010b. Multi-temporal monitoring of wetland water levels in the Florida Everglades using interferometric synthetic aperture radar (InSAR). Remote Sens. Environ. 114, 2436–2447. https://doi.org/10. 1016/i.rse.2010.05.019.
- Hong, Sang-Hoon, Wdowinski, S., Kim, Sang-Wan, 2010a. Evaluation of TerraSAR-X observations for wetland InSAR application. IEEE Trans. Geosci. Remote Sens. 48, 864–873. https://doi.org/10.1109/TGRS.2009.2026895.
- Jaramillo, F., Brown, I., Castellazzi, P., Espinosa, L., Guittard, A., Hong, S.-H., Rivera-Monroy, V.H., Wdowinski, S., 2018. Assessment of hydrologic connectivity in an ungauged wetland with InSAR observations. Environ. Res. Lett. 13, 024003. https:// doi.org/10.1088/1748-9326/aa9d23.
- Jolivet, R., Grandin, R., Lasserre, C., Doin, M.-P., Peltzer, G., 2011. Systematic InSAR tropospheric phase delay corrections from global meteorological reanalysis data. Geophys. Res. Lett. 38
- Kim, J.-W., Lu, Z., Lee, H., Shum, C.K., Swarzenski, C.M., Doyle, T.W., Baek, S.-H., 2009. Integrated analysis of PALSAR/Radarsat-1 InSAR and ENVISAT altimeter data for mapping of absolute water level changes in Louisiana wetlands. Remote Sens. Environ. 113, 2356–2365. https://doi.org/10.1016/j.rse.2009.06.014.
- Kim, J.-W., Lu, Z., Jones, J.W., Shum, C.K., Lee, H., Jia, Y., 2014. Monitoring Everglades freshwater marsh water level using L-band synthetic aperture radar backscatter.
 Remote Sens. Environ. 150, 66–81. https://doi.org/10.1016/j.rse.2014.03.031.
 Kim, J.-W., Lu, Z., Gutenberg, L., Zhu, Z., 2017. Characterizing hydrologic changes of the
- Kim, J.-W., Lu, Z., Gutenberg, L., Zhu, Z., 2017. Characterizing hydrologic changes of the great dismal swamp using SAR/InSAR. Remote Sens. Environ. 198, 187–202. https:// doi.org/10.1016/j.rse.2017.06.009.
- Kim, S.-W., Wdowinski, S., Amelung, F., Dixon, T.H., Won, J.-S., 2013. Interferometric coherence analysis of the Everglades wetlands, South Florida. IEEE Trans. Geosci. Remote Sensing 51, 5210–5224. https://doi.org/10.1109/TGRS.2012.2231418.
- Li, Z., Cao, Y., Wei, J., Duan, M., Wu, L., Hou, J., Zhu, J., 2019. Time-series InSAR ground deformation monitoring: Atmospheric delay modeling and estimating. Earth Sci. Rev. 192, 258–284
- Liang, C., Agram, P., Simons, M., Fielding, E.J., 2019. Ionospheric correction of InSAR time series analysis of C-band Sentinel-1 TOPS data. IEEE Trans. Geosci. Remote Sens. 57 (9), 6755–6773.
- Lin, S., Gregg, R., 1988. Water Budget Analysis: Water Conservation Area 1. DRE 245. South Florida Water Management District report, West Palm Beach, Fla.
- Lu, Z., Kwoun, O., 2008. Radarsat-1 and ERS InSAR analysis over Southeastern coastal Louisiana: implications for mapping water-level changes beneath swamp forests. IEEE Trans. Geosci. Remote Sens. 46, 2167–2184. https://doi.org/10.1109/TGRS. 2008.917271.
- Lu, Z., Crane, M., Kwoun, O.-I., Wells, C., Swarzenski, C., Rykhus, R., 2005. C-band radar observes water level change in swamp forests. EOS Trans. Am. Geophys. Union 86, 141. https://doi.org/10.1029/2005EO140002.
- Lu, Z., Kim, J.-W., Lee, H., Shum, C.K., Duan, J., Ibaraki, M., Akyilmaz, O., Read, C.-H., 2009. Helmand river hydrologic studies using ALOS PALSAR InSAR and ENVISAT altimetry. Mar. Geod. 32, 320–333.
- McVoy, C., Said, W.P., Obeysekera, J., VanArman, J.A., Dreschel, T.W., 2011. Landscapes and Hydrology of the Predrainage Everglades. University Press of Florida Gainesville.
- Meyer, F., 2010. A review of ionospheric effects in low-frequency SAR—Signals, correction methods, and performance requirements. In: Geoscience and Remote Sensing Symposium (IGARSS), 2010 IEEE International. IEEE, pp. 29–32.
- Meyer, F.J., Chotoo, K., Chotoo, S.D., Huxtable, B.D., Carrano, C.S., 2016. The influence of equatorial scintillation on L-band SAR image quality and phase. IEEE Trans.

- Geosci. Remote Sens. 54, 869-880.
- Mitsch, W.J., Bernal, B., Nahlik, A.M., Mander, Ü., Zhang, L., Anderson, C.J., Jørgensen, S.E., Brix, H., 2013. Wetlands, carbon, and climate change. Landsc. Ecol. 28, 583–597.
- Murray, K.D., Bekaert, D.P., Lohman, R.B., 2019. Tropospheric corrections for InSAR: statistical assessments and applications to the Central United States and Mexico. Remote Sens. Environ. 232, 111326.
- Palaseanu, M., Pearlstine, L., 2008. Estimation of water surface elevations for the Everglades, Florida. Comput. Geosci. 34, 815–826. https://doi.org/10.1016/j.cageo. 2007.08.004
- Pearlstine, L., Higer, A., Palaseanu, M., Fujisaki, I., Mazzotti, F., 2007. Spatially continuous interpolation of water stage and water depths using the Everglades Depth Estimation Network (EDEN). (IFAS CIR1521).
- Richards, J.A., Woodgate, P.W., Skidmore, A.K., 1987. An explanation of enhanced radar backscattering from flooded forests. Int. J. Remote Sens. 8, 1093–1100.
- Sklar, F.H., Chimney, M.J., Newman, S., McCormick, P., Gawlik, D., Miao, S., McVoy, C., Said, W., Newman, J., Coronado, C., 2005. The ecological-societal underpinnings of Everglades restoration. Front. Ecol. Environ. 3, 161–169.
- Villa, J.A., Bernal, B., 2018. Carbon sequestration in wetlands, from science to practice: an overview of the biogeochemical process, measurement methods, and policy framework. Ecol. Eng. 114, 115–128.
- Wdowinski, S., 2004. Space-based measurements of sheet-flow characteristics in the Everglades wetland, Florida. Geophys. Res. Lett. 31, L15503. https://doi.org/10. 1029/2004GL020383.
- Wdowinski, S., Amelung, F., Miralles-Wilhelm, F., Dixon, T.H., Carande, R., 2004. Space-based measurements of sheet-flow characteristics in the Everglades wetland, Florida.

- Geophys. Res. Lett. 31.
- Wdowinski, S., Kim, S.-W., Amelung, F., Dixon, T.H., Miralles-Wilhelm, F., Sonenshein, R., 2008. Space-based detection of wetlands' surface water level changes from L-band SAR interferometry. Remote Sens. Environ. 112, 681–696. https://doi.org/10.1016/j.rse.2007.06.008.
- Wegnüller, U., Werner, C., Strozzi, T., Wiesmann, A., Frey, O., Santoro, M., 2016. Sentinel-1 support in the GAMMA software. Procedia Computer Science 100, 1305–1312.
- Werner, C., Wegmüller, U., Strozzi, T., Wiesmann, A., 2002. Processing strategies for phase unwrapping for INSAR applications. In: Proceedings of the European Conference on Synthetic Aperture Radar (EUSAR 2002), pp. 353–356.
- Yu, C., Penna, N.T., Li, Z., 2017. Generation of real-time mode high-resolution water vapor fields from GPS observations. J. Geophys. Res.-Atmos. 122, 2008–2025.
- Yu, C., Li, Z., Penna, N.T., 2018a. Interferometric synthetic aperture radar atmospheric correction using a GPS-based iterative tropospheric decomposition model. Remote Sens. Environ. 204, 109–121.
- Yu, C., Li, Z., Penna, N.T., Crippa, P., 2018b. Generic atmospheric correction model for Interferometric synthetic aperture radar observations. J. Geophys. Res. Solid Earth 123, 9202–9222.
- Yuan, T., Lee, H., Jung, H.C., Aierken, A., Beighley, E., Alsdorf, D.E., Kim, D., 2017.
 Absolute water storages in the Congo River floodplains from integration of InSAR and satellite radar altimetry. Remote Sensing of Environment 201, 57–72.
- Zhang, M., Li, Z., Tian, B., Zhou, J., Tang, P., 2016. The backscattering characteristics of wetland vegetation and water-level changes detection using multi-mode SAR: a case study. Int. J. Appl. Earth Obs. Geoinf. 45, 1–13.